

# Seismic Response of Geocell Retaining Walls: Experimental Studies

Hoe I. Ling<sup>1</sup>; Dov Leshchinsky<sup>2</sup>; Jui-Pin Wang<sup>3</sup>; Yoshiyuki Mohri<sup>4</sup>; and Arik Rosen<sup>5</sup>

**Abstract:** This paper summarizes the seismic response of five large-scale retaining walls having a geocell facing. The walls were 2.8 m high and the backfill and foundation soil were a fine sand compacted to 90% standard Proctor density (relative density of 55%). The first two walls were of the same geometry, with a tapered facing made of geocells each of height 20 cm, one infilled with gravel and the other with sand. In Wall 3, a facing of depth 60 cm was constructed while the backfill sand was reinforced with a polyester geogrid. Wall 4 was similar to Wall 3 except that the backfill was reinforced with several geocell layers. Wall 5 had thin geocell layers of 5 cm height as reinforcements in order to improve the performance compared with Wall 4. The walls were subjected to the scaled horizontal and vertical motions as recorded during the 1995 Kobe earthquake, 4.5 m/s<sup>2</sup> (450 gal) and 9.0 m/s<sup>2</sup> (900 gal) maximum horizontal accelerations in the first and second excitations, respectively. In an attempt to induce failure, and therefore, to investigate the failure mechanism, Walls 3–5 were subjected to a third shaking in which the horizontal accelerations were scaled to 12.0 m/s<sup>2</sup> (1,200 gal). The walls were fully instrumented with accelerometers, laser displacement transducers, force transducers, and strain gauges. All five walls performed satisfactorily under the simulated earthquake motions. An improved wall performance was seen with the geocells acting as reinforcement layers. The study showed that geocells can be used successfully to form gravity walls as well as reinforcement layers even when subjected to a very high seismic load beyond that of the Kobe earthquake.

**DOI:** 10.1061/(ASCE)1090-0241(2009)135:4(515)

**CE Database subject headings:** Seismic effects; Earthquakes; Retaining walls; Experimentation.

## Introduction

The mechanism of soil reinforcement under static loading conditions, such as that due to self-weight and surcharge, has been interpreted as due to pseudocohesion (Schlosser and Long 1973) or increase in confining pressure (Yang 1972). Although successful performance of reinforced soil structures has been reported under earthquake loading [see Ling et al. (1997); Ling and Leshchinsky (1998); Tatsuoka et al. (1998) for a list of case histories], the mechanism of reinforcement has not been widely discussed.

The behavior of reinforced soil composite under earthquake loading can be understood by referring to the deformation of a soil element (Fig. 1) subjected to a constant overburden pressure. During an earthquake, the vertical and horizontal normal stresses remain constant, but cyclic simple shear stresses are induced with alternating positive and negative values (for simplicity, the verti-

cal acceleration is not considered). As can be seen in Fig. 1, the shear stress induced by the earthquake enlarges the Mohr circle or increases the principal stress difference, thus bringing the soil close to a failure state. A sufficiently large shear stress would have brought the circle to touch the failure envelope or induced tension as the minor principal stress becomes zero. Since granular soil does not sustain tensions, cracks will be seen in the soil, especially at the ground surface where the confining stress is very low. The surface cracking during shaking has been reported by Ling et al. (2005a). It is also noticed that with the alternating positive and negative shear stresses, the principal stress that is vertical under static conditions will start to rotate between positive and negative inclinations. The shear strength of soil may be affected by the principal stress rotation (e.g., Ishihara 1996).

The role of tensile reinforcement is to restrain the earthquake-induced shear deformation in soil (Fig. 2). For a soil element that is included between two planar reinforcement layers, such a restraining effect is seen since soil deformation is restrained through the tensile properties of the reinforcements, especially if the reinforcements are closely spaced. Of course, the behavior is affected by the frictional interaction between the reinforcements and soil, as well as the stiffness and strength of reinforcement layers. With a rigid wall facing, such as that constructed from modular blocks, the shear deformation in the soil also is restrained.

Polymeric sheets manufactured from medium- to high-density polyethylene may be welded ultrasonically to create geocells (Fig. 3). Geocells function as three-dimensional soil confinement systems. The geocells are collapsible and can be transported easily to the site, expanded and filled with different types of soils. They were first used to increase the bearing capacity of sand roads for military vehicles (Webster 1979). Since then, geocells have been

<sup>1</sup>Professor, Dept. of Civil Engineering and Engineering Mechanics, Columbia Univ., 500 West 120th Street, New York, NY 10027. E-mail: hil9@columbia.edu

<sup>2</sup>Professor, Dept. of Civil and Environmental Engineering, Univ. of Delaware, Newark, DE 19716.

<sup>3</sup>Graduate Research Assistant, Dept. of Civil Engineering and Engineering Mechanics, Columbia Univ., 500 West 120th Street, New York, NY 10027.

<sup>4</sup>Manager, Geotechnical Laboratory, National Institute of Rural Engineering, 2-1-6 Kannodai, Tsukuba 305-8609, Japan.

<sup>5</sup>Formerly, PRS-Mediterranean, Tel Aviv, Israel.

Note. Discussion open until September 1, 2009. Separate discussions must be submitted for individual papers. The manuscript for this paper was submitted for review and possible publication on October 1, 2007; approved on June 17, 2008. This paper is part of the *Journal of Geotechnical and Geoenvironmental Engineering*, Vol. 135, No. 4, April 1, 2009. ©ASCE, ISSN 1090-0241/2009/4-515–524/\$25.00.

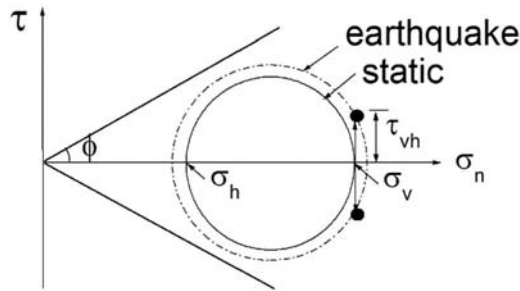
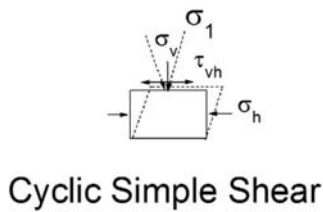


**Fig. 1.** Cyclic simple shear loading

used for different civil engineering applications, including earth retaining walls, slope, embankment, pavement and erosion control. The application of geocells to retaining walls is relatively new (see, for example, Bathurst and Crowe 1994) compared with other polymeric geogrids. A three-dimensional cellular structure such as a geocell restrains further the shear deformation in the soil by “locking” the soil unit in place (for configuration and layout of geocells in a retaining wall, refer to Figs. 3 and 8). The stiffness and strength of the geocells should play an important role in ensuring such restraining effects. Note that while shear deformations are restrained locally by the geocells, the sliding and overturning stabilities of the geocell layers have to be secured in maintaining the global stability of the whole wall system.

In this study, the seismic performance of several soil retaining walls having a geocell facing is investigated using shake table tests. Five soil retaining walls, two with geocell facing alone and three of which included geocells or geogrids as reinforcements,

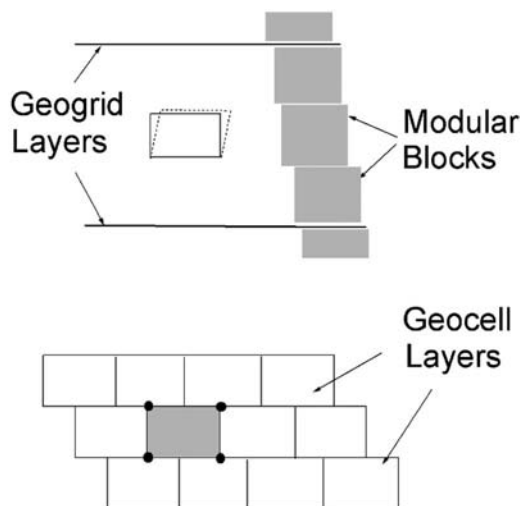


**Fig. 2.** Shear restraining effects in reinforced soil walls

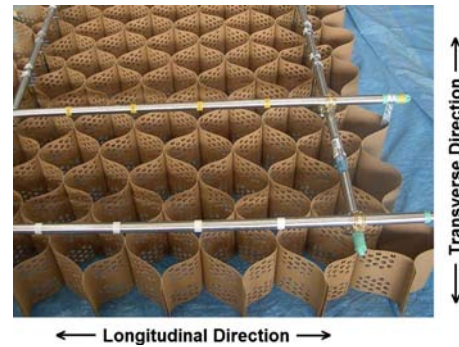


**Fig. 3.** Three-dimensional cellular confinement systems (geocells)

were tested using a total of two or three different shaking intensities by scaling the Kobe earthquake records. The behavior of the walls due to different effects, such as the infill materials and layouts, are presented and discussed.

### Testing Facilities and Input Motions

A three-dimensional shake table of plan dimensions  $6\text{ m} \times 4\text{ m}$  was used for conducting this study. A steel box was fabricated to accommodate a wall of height of 2.8 m (and 0.2 m foundation), length of 4 m, and width of 2 m. The box was mounted firmly to the table. Note that this box was different from the box used in a previous study by Ling et al. (2005a). One of the side walls of the steel box was made detachable to allow for visualization of the entire cross section at the end of testing. The steel frames were used as fixtures for the laser displacement transducers mounted in the front and on top of the wall. The inner sides of the box were polished, lubricated with grease and plastic sheets to minimize friction. Expanded polystyrene (EPS) foam (5 cm thick) were placed at the back and front ends of the steel box to prevent the reflective wave from propagating from the steel box into the backfill.

Part of the north–south (NS) and up–down (UD) components of the 1995 Kobe earthquake accelerations (peak values of 0.59 and 0.34g, respectively, as recorded by the Japan Meteorological Agency), were used in the testings. The Kobe earthquake was a significant event of magnitude 7.2; thus, the records may represent one of the worst case scenarios. A series of parametric studies where the stresses and deformations resulting from different earthquake records were compared showed that the Kobe earthquake records affected most significantly the wall performance (Ling et al. 2005b).

A total of five walls were tested in which the first two walls were subjected to two shakings, whereas the three other walls were subjected to three shakings of different intensities. The peak horizontal accelerations were scaled to 4.5, 9.0, and  $12.0\text{ m/s}^2$  (450, 900, and 1,200 gal) of the recorded values during the first, second, and third shakings, respectively. The vertical accelerations were scaled accordingly. Table 1 summarizes the maximum horizontal and vertical accelerations recorded on the table during each shaking. Note that the resulting wave forms of accelerations of the table were affected by the mass and response of the walls, which were different in all cases, although the table had been calibrated beforehand against the anticipated load. Fig. 4 shows the NS and UD accelerations of the shake table during the second shaking for Wall 5. The input spectra of the three shakings show

**Table 1.** Peak Values of Horizontal and Vertical Accelerations (Unit:  $m/s^2$ )

Wall number	First shaking		Second shaking		Third shaking	
	Horizontal	Vertical	Horizontal	Vertical	Horizontal	Vertical
1	4.53	2.10	8.99	4.12	—	—
2	4.68	2.01	9.26	3.84	—	—
3	4.51	1.99	9.18	3.83	11.86	4.57
4	4.61	1.93	9.27	3.67	11.93	4.69
5	4.04	1.77	8.51	3.33	11.85	4.89

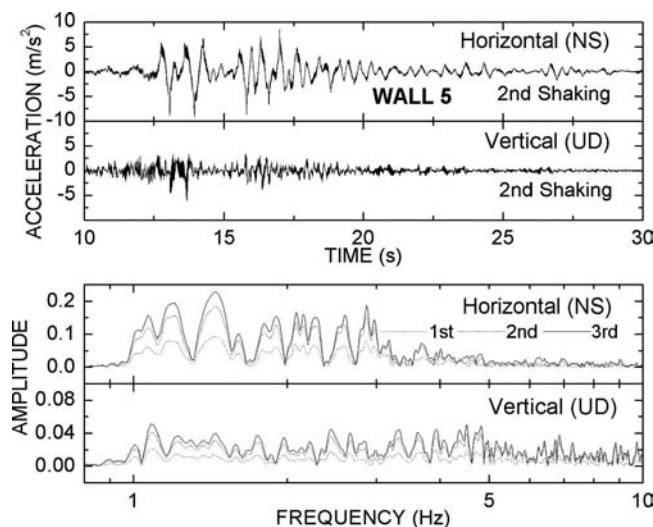
that the frequency contents of the input waves were preserved in the scalings.

## Materials

### Geocells

The geocells (Fig. 3) used in this series of shake table tests were manufactured from high-density polyethylene (HDPE) sheets, each having a thickness of 1.2 mm and height of 20 cm (in Wall 5, the height of the geocell was 5 cm), ultrasonically welded together at seven spots at each seam. Each cell was approximately cylindrical in shape with a radius of 20 cm when filled with soil. The geocells were perforated with holes of 1.5 cm diameter. The surface of the cell was textured in order to improve its interaction with the soil.

The strengths of the unfilled geocell along the longitudinal and transverse directions were measured (Fig. 5). Tensile tests in the transverse direction were conducted using a single cell or multiple cells. They yielded identical results of 10 kN per cell (two HDPE sheets), or average strength of 50 kN/m for the geocells. The seams control the geocell strength along the longitudinal direction. Peel shear tests were conducted on the seams of the geocell. The seam gave a strength of 10 kN per cell that was identical to the strength of a single geocell, since failure occurred on the parent polyethylene sheets surrounding the welded spots. For the geocell having a height of 5 cm, the strength was 12.5 kN/m (i.e., 25% of that of the 20-cm geocell).

**Fig. 4.** Input accelerations and spectra of the 1995 Kobe earthquake

### Sand and Gravel

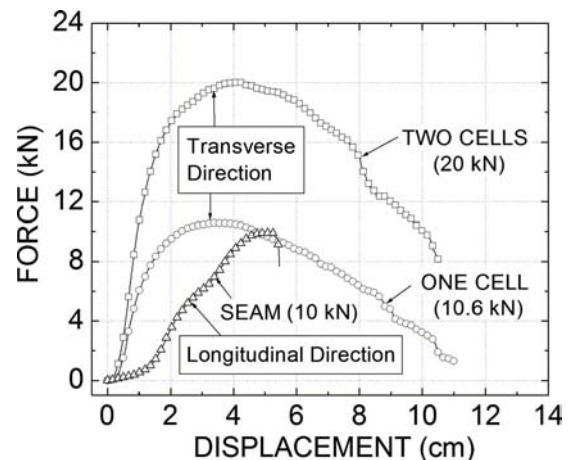
A fine uniform sand (mean diameter,  $D_{50}=0.27$  mm) was used in this study. It was obtained from Tokachi Port in Hokkaido, Japan. The properties of the sand have been studied and reported elsewhere (Ling et al. 2005a). Gravel ( $D_{50}=6$  mm) was used to fill the geocells. It was a commercial product of graded crushed stone M-30 (maximum size up to 35 mm), typically, used as road base material in Japan. The grain-size distributions of the sand and gravel are shown in Fig. 6.

The sand was compacted in the wall to a unit weight of  $15.6$  kN/m<sup>3</sup> or relative density of about 55%. The angle of internal friction of the sand determined from the triaxial compression tests was  $38^\circ$ . The gravel was compacted to an average unit weight of  $20$  kN/m<sup>3</sup>. The triaxial strength of the gravel was not measured since it required a large-scale device, but it should be well above  $50^\circ$ , as Kawabata et al. (2006) measured an angle of internal friction of  $52^\circ$  for a M-25 gravel.

A thin layer of white sand, lighter in color than the backfill sand, was used to create thin narrow seams (5 mm thick, 5 cm wide) in the backfill. The seams allow visualization of the failure surface and differential movements as the backfill is exhumed. The very small volume of seam sand should not have any effect on the backfill properties.

### Soil–Geocell Interactions

A large direct shear device (Matsushima et al. 2007) was used to investigate the interface behavior under constant normal stress. The device was featured with a feedback control and electropneumatic transducers to prevent tilting of the upper box and also to

**Fig. 5.** Tensile properties of geocell in longitudinal and transverse directions

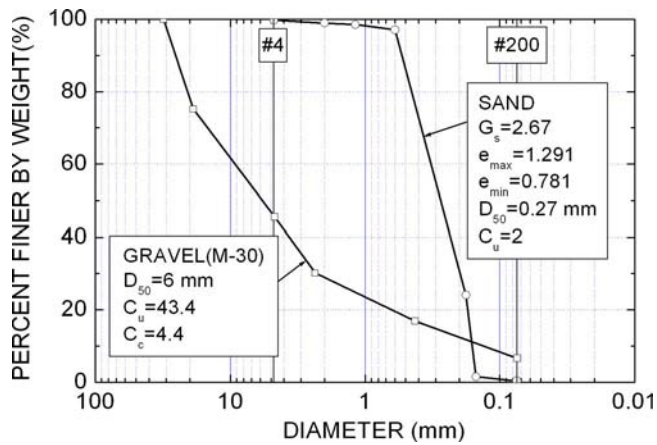


Fig. 6. Grain-size distribution of sand and gravel

maintain a constant normal stress during shearing. This direct shear device had upper and lower shear boxes each of 30-cm height, and length and width of 80 and 50 cm, respectively. The geocell specimen used in the test was composed of four cells in the longitudinal direction and two cells in the transverse direction. The bottom geocell layer thus rested on a 10-cm sand or gravel layer, whereas the top geocell layer was covered by a 10-cm soil or gravel layer. The soil was compacted to the same density as that used in the shake table tests. Four different types of interface were used in the study: a geocell with gravel infill, a geocell with sand infill, a geocell with gravel and a geogrid at the interface, and a geocell with sand and a geogrid at the interface.

Because of the scale and the elaborated testing procedures, all interface tests were conducted at a normal stress of 50 kPa, except the interface of the geocell filled with sand, where an additional test was conducted at a normal stress of 20 kPa in order to validate the linearity of the failure envelope. Note that the friction angle between the polymer sheet and sand, obtained using a modified direct shear device (Ling et al. 2008) was 26.8° (normal stresses ranging between 50 and 95 kPa).

Fig. 7(a) shows the shear stress ratio versus horizontal displacement relationships. The test results [Fig. 7(b)] confirmed that the interaction behavior of sand obeyed the Coulomb law and it was frictional in nature (i.e., the failure envelope was linear and it passes through the origin). Thus, the Coulomb law was assumed for the other interfaces. The friction angle is determined as  $\delta = \tan^{-1} \tau_f / \sigma_{nf}$ , where  $\tau_f$  and  $\sigma_{nf}$  are the average shear and normal stresses at failure, respectively. The geocells infilled with sand, with and without a geogrid, gave very close friction angles of 36.6 and 35.5°, respectively. They attained peak strength (critical state) in about 20-mm displacement. The geocells infilled with gravel, with and without a geogrid layer, showed a hardening behavior, and did not reach a critical state. The friction angles determined at 35-mm displacement were 39.7 and 39.3°, respectively, with and without a geogrid. Thus, the use of gravel as an infill material rendered a larger strength compared to that of sand. The effect of the geogrid layer on the interface strength was negligibly small for the infill with sand or gravel.

### Geogrid

The geogrid was manufactured from polyester and had a strength of 35 kN/m. The mass per unit area was 237 g/m<sup>2</sup> and the aperture size was 2.0 cm. The mechanical properties of this geogrid have been reported by Ling et al. (1998, 2005a). The tensile be-

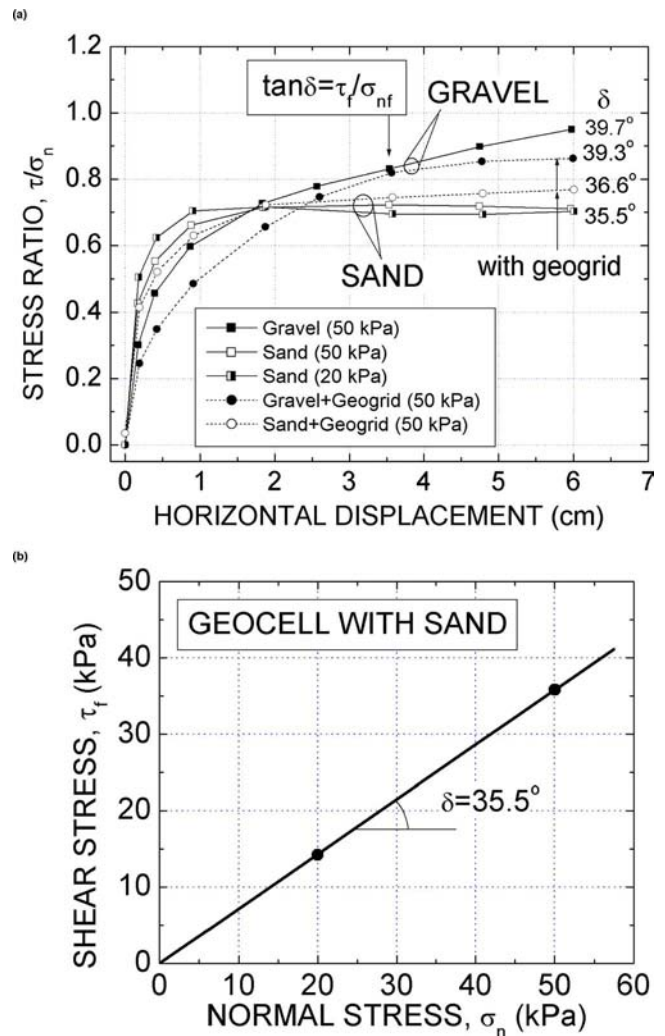


Fig. 7. Direct shear behavior of geocell with different interfaces: (a) shear stress versus displacement; (b) sand interface

havior is independent of the loading rate. Large deformation strain gauges were used to measure the local strains along the length of the geogrid. The strain gauges were protected by rubber silicon sealant. The local strain and corresponding tensile load in the geogrid has been calibrated through the tensile tests.

### Wall Layouts and Instrumentations

Fig. 8 shows the wall layouts. All walls were 2.8 m high, except Wall 5, which was 2.7 m because of the use of both 20- and 5-cm geocell layers. In all the walls, based on the conclusions of previous studies (Ling et al. 2005a), a long top geocell layer of 12 units was provided in order to improve the earthquake performance by inhibiting surface cracks.

Walls 1 and 2 were basically gravity retaining walls with geocell facing. The facing was tapered, with seven geocell units at the bottom and three units below the top layer. The infill materials were gravel and sand, respectively, for Walls 1 and 2. Note that the backfill material was sand.

Geogrid layers of 205-cm length (73% wall height) were used as reinforcement in Wall 3. The geogrid layers were spaced vertically at 40-cm intervals. Thus, a total of six geogrid layers were used. The facing was of three geocell units throughout the height.

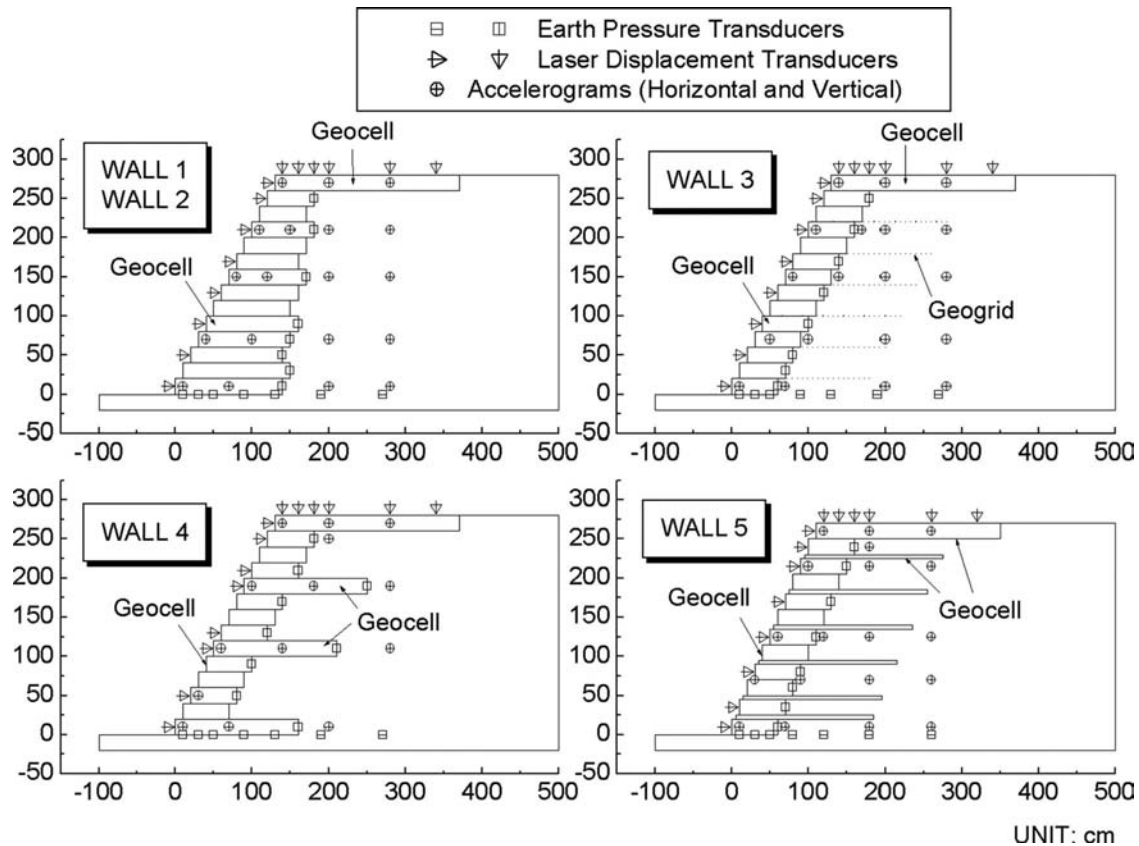


Fig. 8. Wall layouts and instrumentations

Walls 4 and 5 were outgrowths of Wall 3. Instead of using geogrid as reinforcement, geocell layers were used. Three geocell layers (8 units long, 20-cm thick) were placed at a vertical spacing of 80 cm at the bottom of the wall and 60 cm for the top two layers. In Wall 5, geocell layers (9 units long, 5-cm thick) were used. The vertical spacing was one cell at the bottom and two cells at the other parts of the wall. Note that while the facing of Walls 3–5 was infilled with gravel, the portion of geocell extending behind the backfill was filled with sand.

A hand-operated 60-kg compactor was used to construct the backfill in layers of 10 cm thickness. The construction procedures have been documented by Ling et al. (2005a), where a foundation of 20 cm was prepared before the installation of the geocell and backfilling. The geocell facing and layers were also compacted after filling the with soil, which was premixed with a small percentage of moisture. Each geocell layer was placed with an offset of 10 cm in the front, creating a slope angle of 63.4° (with the horizontal). Fig. 9 shows the front view of Wall 3 at the completion of construction.

A total of eight laser displacement transducers were used to measure the lateral displacements of the facing along the height of the wall. The settlements at the crest and foundation were measured using another eight laser displacement transducers. The markers were placed above the backfill for tracing the lateral displacements using a video camera placed from above the wall. A total of seven earth pressure transducers were placed at the foundation to measure the vertical stress in the backfill. A set of 40 accelerometers (20 for horizontal and 20 for vertical accelerations) were placed at designated locations (in front of the facing, behind the facing, in the front and back ends of the backfill) in measuring the accelerations. Eight earth pressure transducers also

were installed at designated locations behind the facing to measure the lateral earth pressure. In Wall 3, eight strain gauges were used to measure the elongation along the length of the geogrid layers. A total of six geogrid layers were instrumented with strain gauges. Note that the strains in the geocell layers were not instrumented.

The data were logged at an interval of 1 min during construction. During shaking, the logging interval was 0.002 s. After the shakings, an additional week was spent to demolish the wall while carefully examining the deformation and slip surfaces.



Fig. 9. Typical front view of wall (Wall 3)



**Fig. 10.** Surface settlements and cracks in Wall 3 after the third shaking: (a) settlement behind the long geocell layer; (b) differential settlement between the geocell facing and backfill; (c) surface cracking in the backfill; and (d) surface cracking in the backfill after the second shaking

## Experimental Results and Discussions

The visual observation of the walls after the shakings as well as the slip surfaces in the backfill have been reported by Leshchinsky et al. (2009). Visually no surface crack or distress was observed on the wall surface after the first shaking. After the second shaking, slight differential settlement between the facing and backfill was observed, with the cracks developed behind the backfill. There was significantly less deformation in Wall 5 compared with the other walls. Following the third shaking (Walls 3–5), the differential settlement increased and more cracks developed (for example, Wall 3, Fig. 10). The shakings did not lead to collapse of the walls. It has to be noted that the observed cracks were at the surface, which were due to the shear stress induced in the soil under very low confining stress. The slip surface initiated behind the top geocell layer. Using the limit equilibrium approach, Leshchinsky et al. (2009) analyzed the test results by back-calculating the seismic coefficients associated with the stability of these walls.

### Lateral Deformations of Wall Facing

It is most useful to assess the wall performance through deformations: facing lateral displacements and crest settlements. The pro-

files of displacements during shakings, at peak and residual states, are shown in Figs. 11(a and b), respectively. During the first shaking, the lateral deformations of the five walls were uniform and negligibly small, in the range of 2–6 mm. Except for the wall reinforced by the geogrid (Wall 3), the deformations in the walls with geocell layers (Walls 4 and 5) were smaller than those having a geocell facing alone (Walls 1 and 2). Note that the geocell facing in the reinforced walls (three geocell units) was smaller than that of the unreinforced walls. The difference in the lateral deformations also was seen during the second shaking. Although the geocell and geogrid reinforced walls (Walls 3–5) showed slightly larger deformations compared with the unreinforced walls (Walls 1 and 2), Wall 5 that was reinforced with closely spaced 5-cm thick geocell layers yielded the smallest displacement of less than 3 cm. The pattern of deformation changed during the third shaking. The maximum displacement for Wall 4, for example, increased from about 45 to 16 cm. Geogrid reinforced walls showed comparable performance with the geocell reinforced wall (Wall 5). The more openly spaced geocell layers (Wall 4) gave the largest deformation.

Fig. 11(b) shows that the trend of residual deformations was similar to that at peak deformation. The results show that part of the lateral deformation was recovered after shakings. The com-



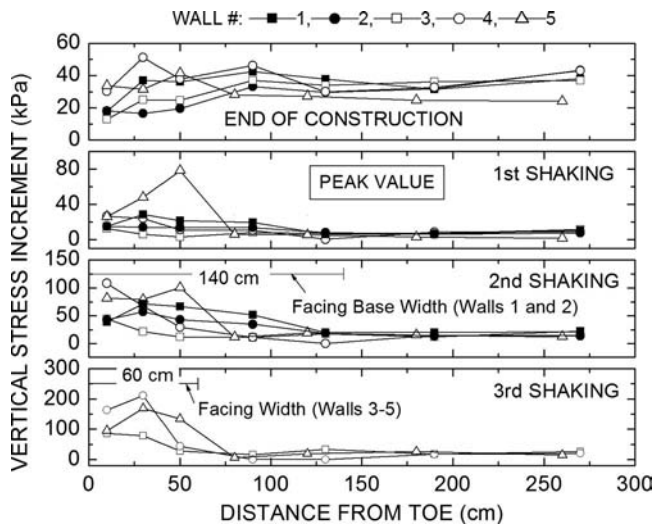


Fig. 14. Vertical stress increments during construction and shakings

for Wall 5 was due to its height of 2.7 m compared with 2.8 m of the other walls. There was variation in the vertical stress at the front end of the walls. The vertical stress at the front of the wall was less than that of the backfill because of the 63.4° slope. Wall 2 had the smallest vertical stress in the front slope because the geocell facing was infilled with sand instead of gravel.

During shaking, the vertical stress increment at peak was larger in the wall front compared with that of the backfill. The results signified that the wall moved, and thus the backfill exerted an increased vertical pressure through the facing as eccentricity load. At the end of shaking, about half of the magnitude of the peak vertical stress remained as residual stress (not shown here).

### Accelerations and Response Spectra

The peak accelerations at different locations were obtained by the transducers. For simplicity, the peak horizontal accelerations at the front of the facing and in the backfill (268 cm from the toe of the wall) are plotted in Figs. 15(a and b), respectively. In general, there was very small amplification of accelerations in the geocell walls. Wall 5 tended to give a bigger amplification at the top compared with the other walls. For the walls subjected to a third shaking, the acceleration attenuated. The amplification factor at the top of the walls, typically, was less than 2 even under the third

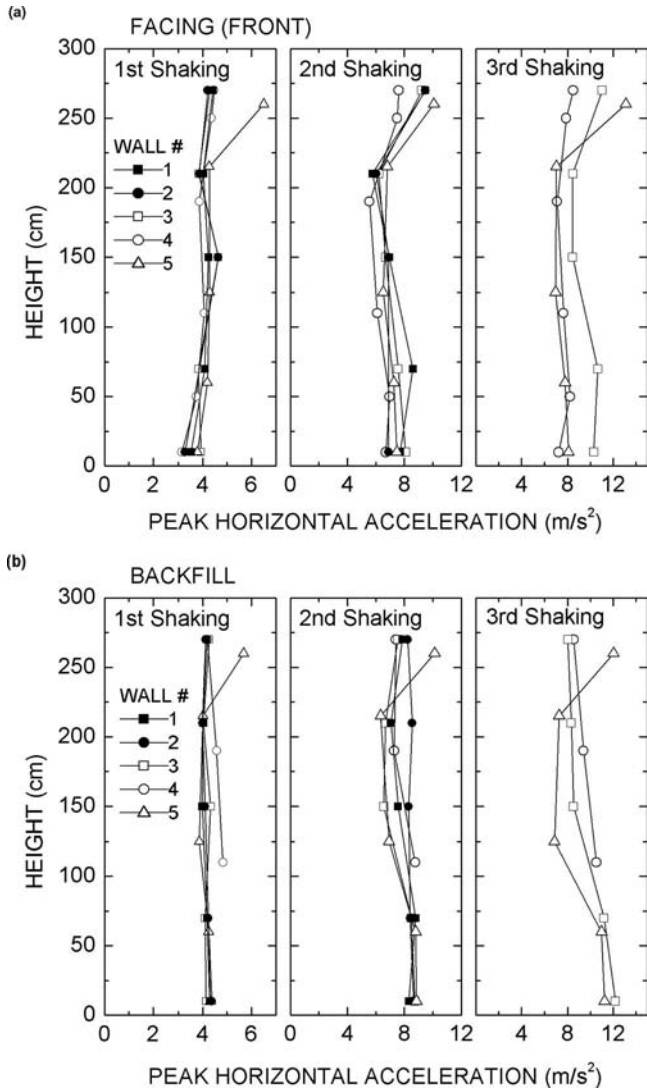


Fig. 15. Maximum wall horizontal accelerations: (a) wall facing; (b) backfill

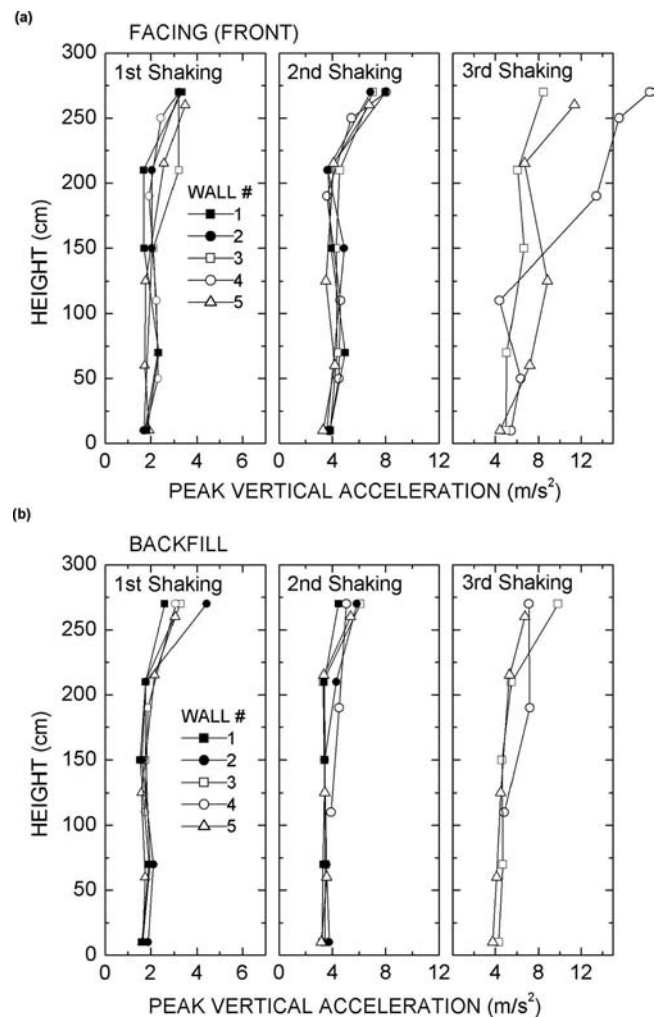


Fig. 16. Maximum wall vertical accelerations: (a) wall facing; (b) backfill

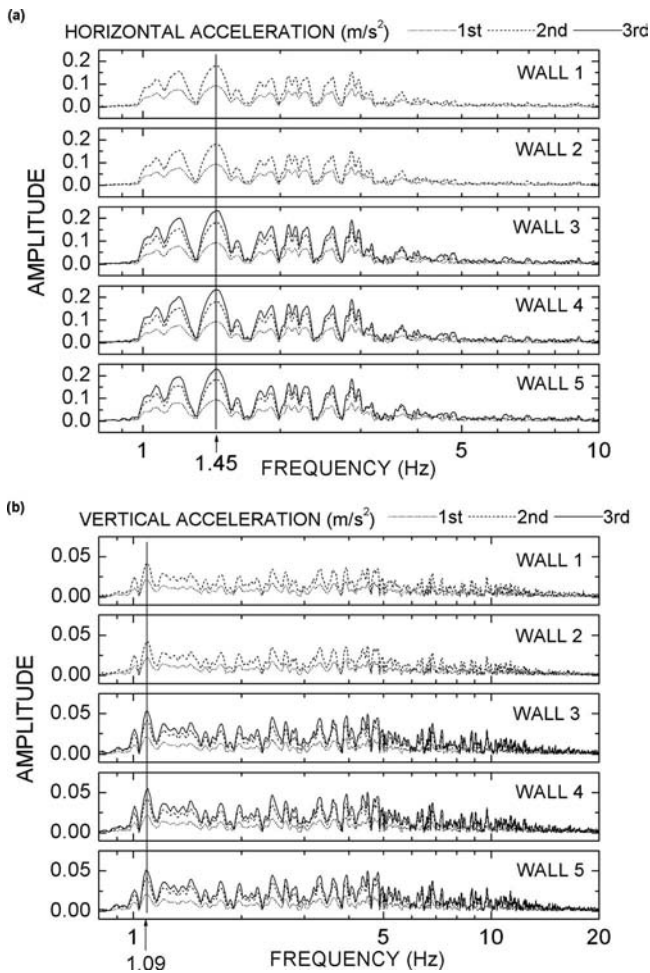


Fig. 17. Response spectra at top of wall: (a) horizontal; (b) vertical accelerations

shaking. The same trend of amplification of vertical acceleration is seen [Figs. 16(a and b)], and this occurred only at the top 70 cm of the wall. The vertical amplification was large at the facing front for Wall 4.

The response spectra for the horizontal and vertical accelerations were obtained through fast Fourier transform. Figs. 17(a and b) show typical results of the response spectra close to the wall top surface. It is interesting to see that the frequency contents did not change during the three shakings throughout the wall. With an increase in acceleration during the second and third shakings, the magnitude increased for all frequency components. The predominant frequency of the wall was 1.45 Hz (period=0.69 s) for the horizontal acceleration and 1.09 Hz (period=0.92 s) for the vertical acceleration.

### Tensile Force in Geogrid

Wall 3 was reinforced with six geogrid layers. The results of the six instrumented layers are shown in Fig. 18. The tensile force developed in the top three geogrid layers was negligibly small. The bottom layer developed a larger tensile force (about 30% the tensile strength) compared with the other layers. The potential slip surface initiated behind the top geogrid layer; thus, their role as tensile reinforcements became more significant at the bottom of the wall.

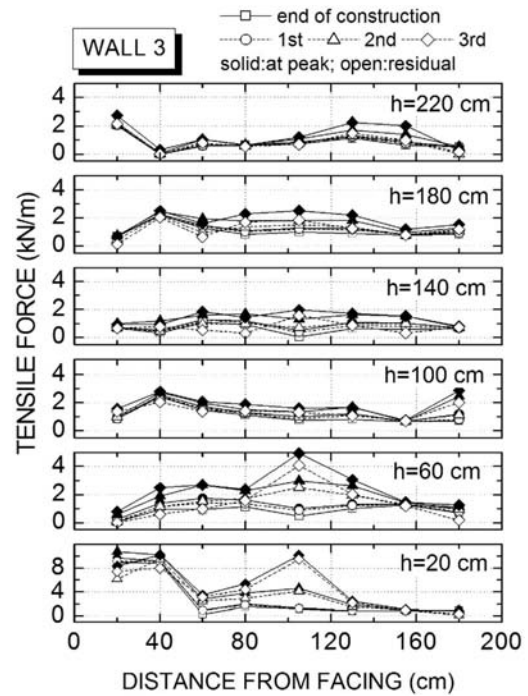


Fig. 18. Tensile force in geogrid layers (Wall 3)

### Discussions

The series of five shake table tests indicated that the soil retaining wall with the geocell facing performed very well under significant earthquake loadings. The acceleration amplification and deformations were negligible after the first shaking and within acceptable values for the second shaking. The walls remained stable after the third shaking where the maximum acceleration was in excess of 1.2 g.

Gravity walls made of geocells are flexible. Their seismic performance is much better than that of rigid (concrete) gravity walls. This is evident by comparing the tested walls (Walls 1 and 2) with the numerous failed concrete gravity walls in the Kobe earthquake (e.g., Tatsuoka et al. 1998). Some of the failed walls were not significantly taller than the tested geocell walls.

The tensile behavior of geocells with infill soil requires further study. So far, only their unfilled tensile properties were measured.

### Conclusions

The major conclusions drawn from this study are:

- The top, long geocell layer successfully restrained the failure surface from developing. Other geocell and geogrid reinforcement layers improved the performance of the wall system. The bottom geogrid layers arrested larger tensile forces compared with the top layers.
- The geocell layers can be used to reinforce, in addition to retaining, the soil. Comparing Walls 3–5, Wall 5 [which was reinforced by closely spaced geocell layers of small thickness (5 cm)] exhibited the best performance.
- The accelerations are in phase throughout the walls for the shakings. The amplification factor at the top of the wall was around 2. The frequency contents of the horizontal and vertical accelerations were similar throughout the walls. The fundamental frequency of the walls was obtained as 1.45 Hz.

- The geocell fill material utilizing gravel performed better in terms of settlement compared with that of sand. The difference in lateral displacement between the walls filled with sand and gravel was negligibly small.
- The lateral earth pressure distribution behind the geocell facing was random. With shakings, load eccentricity was observed under the base of the geocell facing.

It has to be noted that the measured performance was limited to a particular geocell soil retaining wall system. Hence, the results as reported and conclusions should not be extrapolated to other wall systems. Also, the results as reported should be useful for developing and validating numerical procedures in analyzing the seismic behavior of geocell reinforced soil retaining walls.

## Acknowledgments

This study was funded by the PRS-Mediterranean and implemented with the collaborative research agreement between Columbia University and the National Research Institute of Rural Engineering (NRIRE) in the use of shake table facilities. Mutsuo Takeuchi, Kenichi Matsushima, and Mitsuru Ariyoshi of NRIRE provided invaluable support for this study. Yoshikazu Okabe of the Tokyo Soil Research supervised the construction works.

## References

Bathurst, R. J., and Crowe, R. E. (1994). "Recent case histories of flexible geocell retaining walls in North America." *Recent case histories of permanent geosynthetic-reinforced soil retaining walls*, F. Tatsuoka and D. Leshchinsky, eds., Balkema, Rotterdam, The Netherlands, 3–19.

Ishihara, K. (1996). *Soil behavior for earthquake geotechnics*, Oxford University Press, London.

Kawabata, T., Ling, H. I., Mohri, Y., and Shoda, D. (2006). "The behavior of buried flexible pipe under high fills and design implications." *J. Geotech. Geoenviron. Eng.*, 132(10), 1354–1359.

Leshchinsky, D., Ling, H. I., Wang, J.-P., Rosen, A., and Mohri, Y.

(2009). "Equivalent seismic coefficient in geocell retention systems." *Geotext. Geomembr.*, 27(1), 9–18.

Ling, H. I., and Leshchinsky, D. (1998). "Effects of vertical acceleration on seismic design of geosynthetic-reinforced soil structures." *Geotechnique*, 48(3), 347–373.

Ling, H. I., Leshchinsky, D., and Perry, E. B. (1997). "Seismic design and performance of geosynthetic-reinforced soil structures." *Geotechnique*, 47(5), 933–952.

Ling, H. I., Liu, H., and Mohri, Y. (2005b). "Parametric studies on the behavior of reinforced soil retaining walls under earthquake loading." *J. Eng. Mech.*, 131(10), 1056–1065.

Ling, H. I., Mohri, Y., and Kawabata, T. (1998). "Tensile properties of geogrids under cyclic loadings." *J. Geotech. Geoenviron. Eng.*, 124(8), 782–787.

Ling, H. I., Mohri, Y., Leshchinsky, D., Burke, C., Matsushima, K., and Liu, H. (2005a). "Large-scale shaking table tests on modular-block reinforced soil retaining walls." *J. Geotech. Geoenviron. Eng.*, 131(4), 465–476.

Ling, H. I., Wang, J.-P., and Leshchinsky, D. (2008). "Cyclic behavior of soil–structure interfaces in a reinforced soil wall: Experimental studies." *Geosynthet. Int.*, 15(1), 14–21.

Matsushima, K., Mohri, Y., Aqil, U., Yamazaki, S., and Tatsuoka, F. (2007). "Mechanical behavior of reinforced specimen using constant pressure large direct shear test." *Soil stress–strain behavior: Measurement, modeling, and analysis*, H. I. Ling, L. Callisto, D. Leshchinsky, and J. Koseki, eds., Springer, New York, 837–848.

Schlosser, F., and Long, N. T. (1973). "Etude du comportement du materiau terre armee." *Ann. Inst. Tech. Bat. Trav. Publics*, 304, Ser. Mater. No. 45.

Tatsuoka, F., Koseki, J., Tateyama, M., Munaf, Y., and Horii, K. (1998). "Seismic stability against high seismic loads of geosynthetic reinforced soil retaining structures." *Proc., 6th Int. Conf. on Geosynthetics*, Atlanta, Keynote Lecture, 103–142.

Webster, S. L. (1979). "Investigation of beach sand trafficability enhancement using sand-grid confinement and membrane reinforcement concepts." *Technical Rep. GL-79-20*, U.S. Army Corps of Engineers Waterway Experiment Station, Vicksburg, Miss.

Yang, Z. (1972). "Strength and deformation characteristics of reinforced sand." Ph.D. thesis, Univ. of California at Los Angeles, Los Angeles, Calif.